Imaging-Guided Combined Photothermal and Radiotherapy to Treat Subcutaneous and Metastatic Tumors Using Iodine-131-Doped Copper Sulfide Nanoparticles

Xuan Yi, Kai Yang, Chao Liang, Xiaoyan Zhong, Ping Ning, Guosheng Song, Dongliang Wang, Cuicui Ge, Chunying Chen, Zhifang Chai, and Zhuang Liu**

Combining different therapeutic strategies to treat cancer by overcoming limitations of conventional cancer therapies has shown great promise in both fundamental and clinical studies. Herein, by adding ^{131}I when making iodine-doped CuS nanoparticles, CuS/[^{131}I]I nanoparticles are obtained, which after functionalization with polyethylene glycol (PEG) are used for radiotherapy (RT) and photothermal therapy (PTT), by utilizing their intrinsic high near-infrared absorbance and the doped ^{131}I-radioactivity, respectively. The combined RT and PTT based on CuS/[^{131}I]I-PEG is then conducted, achieving remarkable synergistic therapeutic effects as demonstrated in the treatment of subcutaneous tumors. In the meanwhile, as revealed by bimodal nuclear imaging and computed tomography (CT) imaging, it is found that CuS/[^{131}I]I-PEG nanoparticles after being injected into primary solid tumors could migrate to and retain in their nearby sentinel lymph nodes. Importantly, the combined RT and PTT applied on those lymph nodes to assist surgical resection of primary tumors results in remarkably inhibited cancer metastasis and greatly prolonged animal survival. In vivo toxicology studies further reveal that our CuS/I-PEG is not obviously toxic to animals at fourfold of the treatment dose. This work thus demonstrates the potential of combining RT and PTT using a single nanoagent for imaging-guided treatment of metastatic tumors.

1. Introduction

Cancer has become a leading cause of human death. To date, surgery, chemotherapy, and radiotherapy (RT), the latter of which could be further classified into internal RT (with radiation from radionuclide administrated into tumors) and external RT (with externally applied radiation), are still the three mostly adapted strategies for cancer treatment. However, each of those current treatment approaches has its limitations such as toxic side effects and limited therapeutic efficacy.[1,2] In particular, for patients with later stage of cancer when tumor metastasis already happens, traditional treatment strategies would become rather ineffective. During cancer metastasis, sentinel lymph nodes (SLNs) nearby the primary tumor are usually the primary targets of early stage metastasis via the lymphatic pathway.[3,4] Therefore, it is of great importance to identify the locations of SLNs, treat those nodes invaded by metastasis tumor cells, and thus stop further spread of cancer cells to other organs.

Photothermal therapy (PTT) as a minimally invasive therapeutic approach has attracted increasing attention in recent years. Nanomaterials with high near-infrared (NIR) optical absorbance can generate heat under laser irradiation to increase tumor local temperature and ablate cancer cells.[5,6] Various photothermal agents including noble metal nanostructures,[7–14] nanocarbons,[15–17] transition metal sulfide/oxides nanomaterials,[18–22] as well as many organic nanoparticles[23–27] have been explored for cancer PTT. PTT may also be combined with many other different therapeutic strategies such as chemotherapy, gene therapy, photodynamic therapy, and even surgery to realize improved therapeutic outcomes.[6,28–30] In our recent studies, we found that imaging-guided PTT to ablate SLNs nearby the tumor, when conducted together with surgical resection of the primary tumor, is able to prevent lymphatic metastasis of tumor cells.[31,32] Moreover, we have also uncovered that the combination of PTT with immunotherapy could trigger potent immunological responses to kill cancer cells remaining in the body, and thereby inhibit tumor metastasis.[32] However,

X. Yi, Prof. K. Yang, X. Zhong, P. Ning, Prof. C. Ge, Prof. Z. Chai
School of Radiation Medicine and Protection and School for Radiological and Interdisciplinary Sciences (RAD-X) Collaborative Innovation Center of Radiation Medicine of Jiangsu Higher Education Institutions
Medical College of Soochow University
Suzhou, Jiangsu 215123, China
E-mail: kyang@suda.edu.cn

C. Liang, Dr. G. Song, Prof. Z. Liu
Institute of Functional Nano and Soft Materials (FUNSOM) and Collaborative Innovation Center of Suzhou Nano Science and Technology Soochow University
Suzhou, Jiangsu 215123, China
E-mail: zliu@suda.edu.cn

Dr. D. Wang, Prof. C. Chen
CAS Key Laboratory for Biomedical Effects of Nanomaterials and Nanosafety
National Center for Nanoscience and Technology of China
Beijing 100190, China

DOI: 10.1002/adfm.201502003

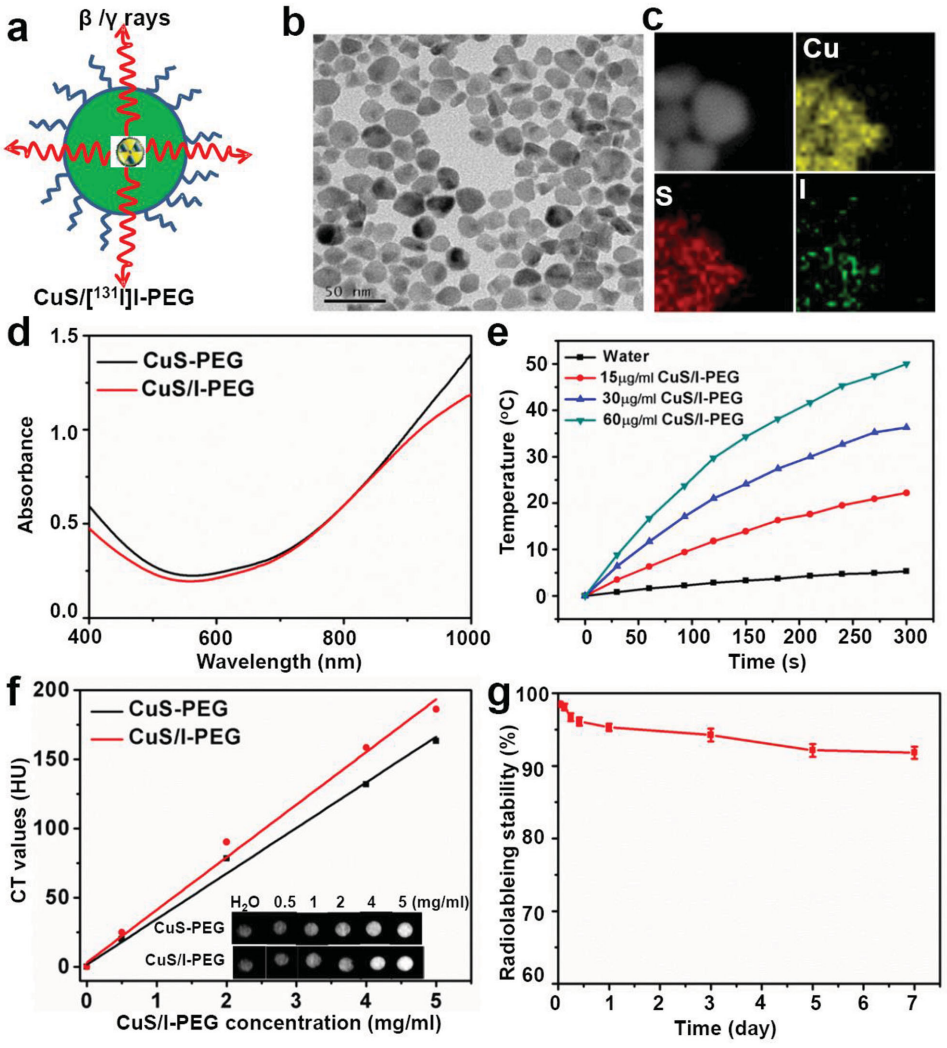

Figure 1. Preparation and characterization of iodine-doped CuS/I nanoparticles. a) Schematic illustration of CuS/[^{131}I]I-PEG nanoparticles. b) TEM images of CuS/I nanoparticles. c) Energy-dispersive X-ray spectroscopy (EDX) elemental mapping of CuS/I nanoparticles showing the existence of I in the obtained nanoparticles. d) UV–vis–NIR spectra of CuS and CuS/I nanoparticles after functionalization with PEG. Iodine doping induced no significant change of CuS absorbance. e) Photothermal heating curves of CuS/I-PEG at different concentrations under 808 nm laser irradiation. f) CT values of CuS/I-PEG and CuS-PEG solutions with different concentrations. Inset: CT images of CuS/I-PEG and CuS-PEG solutions in water. g) The radiolabeling stability of CuS/[^{131}I]I-PEG incubated with mouse plasma at 37 °C.

the combination of PTT with radiotherapy (RT), which relies on the ionization irradiation to damage cancer cells, as well as using such an approach to stop tumor metastasis, has not yet been achieved to our best knowledge.

Copper sulfide (CuS) nanoparticles with strong NIR absorbance have been widely used as a photothermal agent for ablation of cancer cells as well as a contrast agent in photoacoustic imaging.[18,33–41] In addition, CuS nanoparticles could be labeled with radionuclide ^{64}Cu, obtaining [^{64}Cu]CuS nanoparticles suitable for both positron emission tomography (PET) imaging and photothermal cancer treatment.[42,43] In this work, we develop iodine-doped CuS (CuS/I) nanoparticles which are labeled with radionuclide ^{131}I, a commonly used radioisotope in RT, for multimodal imaging-guided combined internal RT and PTT in cancer treatment, showing great efficacy not only to destruct subcutaneous tumors but also to prevent tumor metastasis. CuS/I nanoparticles were synthesized by a simple aqueous phage method at room temperature.[44] By simply introducing ^{131}I during nanoparticle synthesis, we obtained radio-labeled CuS/[^{131}I]I nanoparticles, which were then non-covalently modified with polyethylene glycol (PEG) (**Figure 1**a). Taking advantages of the intrinsic high NIR optical absorbance as well as the radioactivity of CuS/[^{131}I]I-PEG, the combined PTT and internal RT was then conducted on a subcutaneous mouse tumor model by direct injection of CuS/[^{131}I]I-PEG into tumors, which were then exposed to an 808 nm NIR laser with a low power density, achieving a remarkable synergistic therapeutic effect. In a lymph node metastasis model, we further uncovered that CuS/[^{131}I]I-PEG could serve as a contrast agent for both nuclear imaging and X-ray computed tomography (CT) imaging, which revealed effective translocation of nanoparticles from the injected primary tumors to the nearby SLNs. The

combined RT and PTT was then conducted on lymph nodes to assist surgical resection of primary tumors, resulting in remarkably inhibited cancer lung metastasis and greatly prolonged animal survival compared with other groups after the respective monotherapies. Moreover, no obvious toxicity of our CuS/I-PEG nanoparticles at a dose which was fourfold of the treatment dose was observed in our short-term toxicology study. Our work demonstrates the idea of combining photothermal therapy with radiotherapy by a single nanoagent, and shows the promise of using such imaging-guided combined RT and PTT for tumor metastasis treatment.

2. Results and Discussion

In our study, iodine-doped CuS nanoparticles were synthesized in the aqueous solution according to the protocol of making bare CuS nanoparticles with slight modifications.[44] In brief, copper chloride ($CuCl_2$), sodium sulfide (Na_2S), and potassium iodide (KI) were mixed in an aqueous solution at the Cu:S:I molar ratio of 1:0.5:0.1 in the present of sodium citrate upon stirring overnight at room temperature. Excess copper and other unreacted ions were removed by centrifugation. The obtained CuS/I nanoparticles were well-dispersed in water and showed relatively uniform sizes with an average diameter of ≈20 nm (Figure 1b,c, Figure S1, Supporting Information). X-ray-power diffraction (XRD) measurements of CuS/I nanoparticles displayed obvious diffraction peaks of CuS (JCPDS no. 06-0464). No peaks of any other phases were detected, indicating that the crystal structure of CuS nanoparticles after being doped with iodine exhibited no obvious change (Figure S2a, Supporting Information). The existence of iodine in our prepared CuS/I nanoparticles was confirmed by X-ray photoelectron spectroscopy (XPS) (Figure S2b, Supporting Information). Moreover, energy-dispersive X-ray spectroscopy (EDS) mapping of nanoparticles (Figure 1c) suggested that the three elements of Cu, S, and I were uniformly distributed inside our obtained CuS/I nanoparticles.

UV–vis–NIR spectrum of CuS/I nanoparticles showed a broad absorbance band from 700 to 1000 nm, which appeared to be similar to the spectrum of bare CuS nanoparticles (Figure 1d). The as-prepared CuS/I nanoparticles were then functionalized with PEG-grafted poly(maleic anhydride-alt-1-octadecene) (C18PMH-PEG) to improve their water solubility, obtaining PEGylated CuS/I (CuS/I-PEG) nanoparticles with a hydrodynamic diameter of ≈45 nm and excellent stability in various physiological solutions (Figure S3, Supporting Information). We next investigated the photothermal properties of those nanoparticles induced by the NIR laser irradiation. When exposed to an 808 nm laser at the power density of 0.8 W cm^{-2}, CuS/I-PEG nanoparticles exhibited concentration-dependent photothermal heating effect (Figure 1e). Note that the photothermal effect of those nanoparticles may be even stronger if a laser with longer wavelength (e.g. 1064 nm) is used.

X-ray computer tomography (CT) imaging is a widely used imaging technique in the clinic. Interestingly, it was uncovered that CuS/I-PEG nanoparticles could be used as a CT imaging agent owing to their X-ray absorbance ability (Figure 1f). The CT contrast and Hounsfield unit (HU) values of CuS/I-PEG increased linearly with the nanoparticle concentrations (Figure 1f) and were found to be higher than those of bare CuS nanoparticles without iodine doping.

For radionuclide ^{131}I doping, CuS/[^{131}I]I were prepared using the same procedure as for the preparation of plain CuS/I nanoparticles except that a trace amount of $Na^{131}I$ was added. The obtained CuS/[^{131}I]I nanoparticles were then PEGylated and purified by washing with deionized water several times to remove impurity and excess free ^{131}I. To test the radiolabeling stability of CuS/[^{131}I]I-PEG, we incubated those radioactive nanoparticles in mouse plasma at 37 °C, and found minimal amounts of ^{131}I detachment from nanoparticles over 7 d, demonstrating the excellent radiolabeling stability of ^{131}I doped inside those CuS/[^{131}I]I-PEG nanoparticles (Figure 1g). In our experiments, the average ^{131}I labeling yield was ≈34%, based on which the Cu:S:I molar ratio was estimated to be 15.2:14.7:1 in our CuS/[^{131}I]I-PEG nanoparticles.

Before using CuS/I-PEG nanoparticles as therapeutic agent for imaging-guided RT and PTT treatment, we first studied the cellular uptake behaviors of CuS/I-PEG nanoparticles. 4T1 murine breast cancer cells were incubated with fluorescein isothiocyanate (FITC) labeled CuS/I-PEG nanoparticles. After 6 h of incubation, the cells were collected and imaged by a confocal fluorescence microscope. Rather strong green fluorescence signals appeared in the cytoplasm of cells, suggesting the efficient cellular uptake of CuS/I-PEG nanoparticles (**Figure 2**a), which was further confirmed by flow cytometry analysis (Figure 2b). In order to accurately measure the cellular uptake of radioactive isotope, cells were also incubated with CuS/[^{131}I]I-PEG or free ^{131}I at the doses of 10, 20, and 40 μCi for 6 h, washed extensively with PBS, and then collected for gamma counter measurement (Figure 2c). Interestingly, much stronger radioactivity levels were found in cells incubated with CuS/[^{131}I]I-PEG compared to those treated with free ^{131}I, suggesting that ^{131}I in the nanoparticle formulation could be more effectively engulfed by cells.

The in vitro cytotoxicity of CuS/I-PEG with or without ^{131}I doping was then tested. 4T1 cancer cells were incubated with different concentrations of CuS/I-PEG, CuS/[^{131}I]I-PEG, and free ^{131}I for 24 h, and then tested by the cell counting kit-8 (CCK-8) assay. No significant cytotoxicity was observed for cold CuS/I-PEG nanoparticles without ^{131}I labeling in our tested dose range (Figure S4a, Supporting Information). Compared to free ^{131}I, CuS/[^{131}I]I-PEG with the same radioactivity doses showed significantly enhanced cancer cell killing ability (Figure 2d). Such improved RT efficacy delivered by CuS/[^{131}I]I-PEG could be attributed to the dramatically increased cellular uptake of ^{131}I carried by CuS/[^{131}I]I-PEG (Figure 2a,c).

Next, we studied in vitro combined RT and PTT with CuS/[^{131}I]I-PEG nanoparticles. In our experiments, 4T1 cells preincubated with CuS/[^{131}I]I-PEG for 12 h were irradiated by the 808 nm laser (0.8 W cm^{-2} for 5 min), and then incubated for another 12 h before the CCK-8 assay. In marked contrast to RT alone (CuS/[^{131}I]I-PEG without laser) and PTT alone (CuS/I-PEG with laser), which could only partially kill cancer cells under our tested conditions, the combined RT and PTT (CuS/[^{131}I]I-PEG with laser) offered greatly enhanced cancer cell killing efficacy (Figure 2e, Figure S5, Supporting Information). Cancer cells with the combination therapy were almost

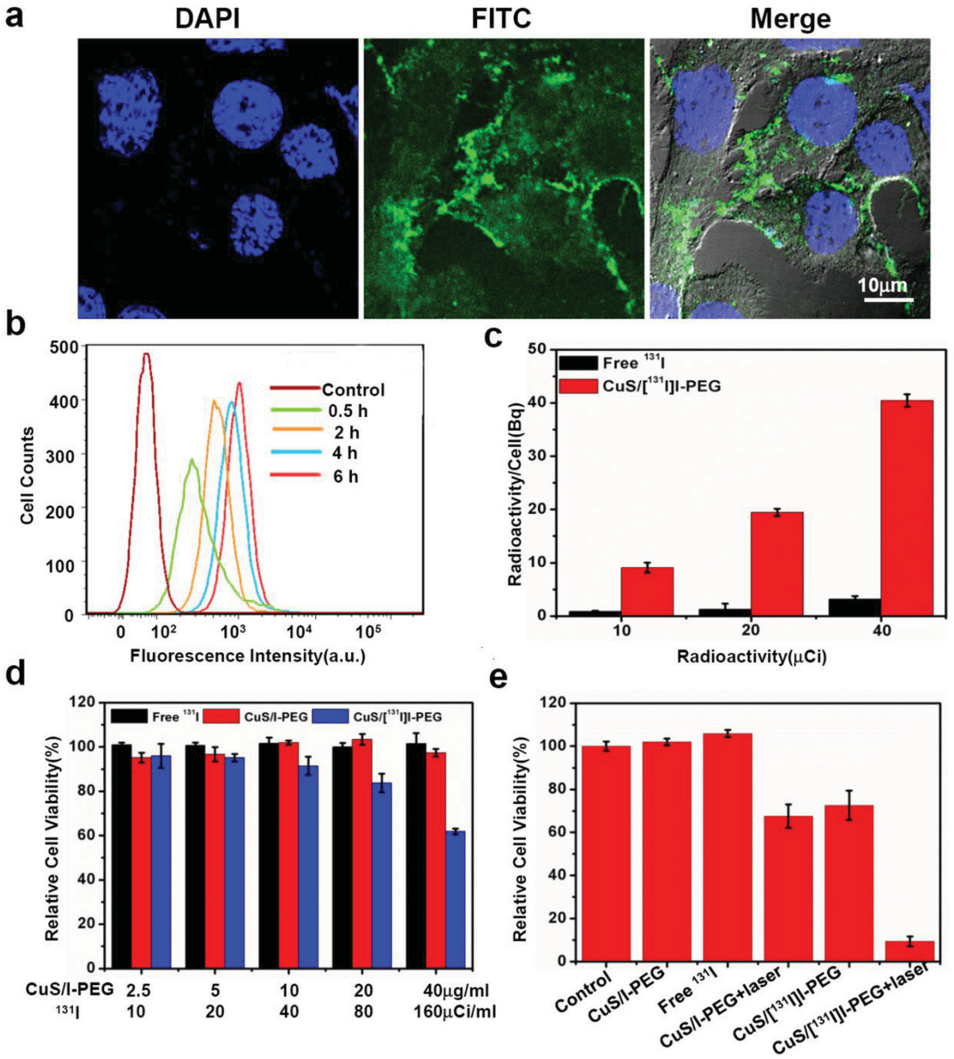

Figure 2. In vitro cell experiments. a) Confocal fluorescence images of 4T1 cells incubated with 30 μg mL^{-1} FITC-labeled CuS/I-PEG for 6 h. b) Flow cytometry measurement of FITC fluorescence intensities in 4T1 cells after 0.5, 2, 4, and 6 h of incubation with CuS/I-PEG-FITC. c) Cell uptake of free ^{131}I and CuS/[^{131}I]I-PEG at the different concentrations of radioactivity. d) The relative viabilities of 4T1 cells incubated with different concentrations of CuS/I-PEG, free ^{131}I, and CuS/[^{131}I]I-PEG. e) The in vitro combination of RT and PTT treatment for 4T1 cells.

completely destructed, a result of a synergistic effect which appeared to be obviously stronger than a simple additive effect.

Motivated by the excellent efficacy achieved by in vitro combination therapy, we then studied the in vivo combined RT and PTT on a subcutaneous mouse tumor model. Balb/c mice bearing 4T1 tumors were randomly divided into six groups in our experiments. For combination therapy, mice were intratumorally injected with CuS/[^{131}I]I-PEG (dose = 5 mg kg^{-1}, 50 μCi of ^{131}I per mouse) and then irradiated by the 808 nm laser (0.25 W cm^{-2}, 20 min). Other control groups of mice (five mice per group) included untreated mice, mice with free ^{131}I injection, mice with CuS/I-PEG injection with or without laser irradiation, and mice with CuS/[^{131}I]I-PEG injection but no laser irradiation.

As monitored by an infrared (IR) thermal camera, tumors injected with CuS/I-PEG could be effectively heated under the NIR laser irradiation at a rather low power density (0.25 W cm^{-2}), with their surface temperatures kept at ≈45 °C for 20 min (**Figure 3**a,b). Such a mild hyperthermia treatment, however, by itself was not able to delay the tumor growth (Figure 3c). As for RT alone, consistent to our in vitro results, CuS/[^{131}I]I-PEG rendered better therapeutic efficacy compared to free ^{131}I at the same radioactivity dose (50 μCi per mouse), possibly because of the enhanced cell uptake and prolonged tumor retention of radionuclide ^{131}I in the nanoparticles formulation after being injected into tumors. Unfortunately, such effect still was only able to slightly delay the tumor growth (Figure 3c). In marked contrast, in the combination therapy group, the tumors injected with CuS/[^{131}I]I-PEG after laser irradiation showed significantly inhibited growth, and became much smaller than tumors in other control groups (Figure 3c,d). Terminal deoxynucleotidyl transferase dUTP nick end labeling (TUNEL) staining of tumor slices (Figure 3e) further confirmed that combination of RT and PTT based on CuS/[^{131}I]I-PEG nanoparticles could induce tumor cell apoptosis

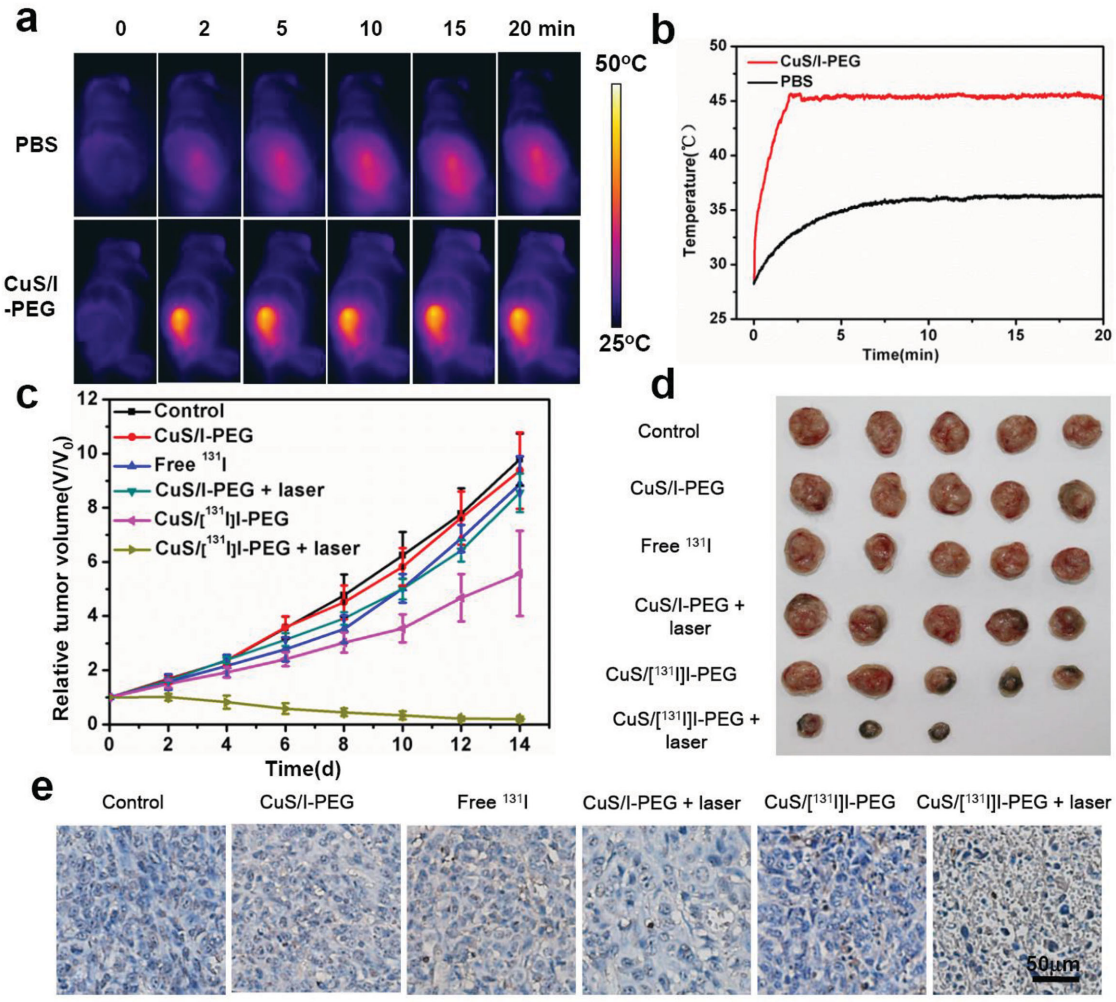

Figure 3. In vivo combined internal RT and PTT for treatment of subcutaneous tumors. a) IR imaging of mice injected with CuS/I-PEG or PBS under the 808 nm laser irradiation at 0.25 W cm^{-2} for 20 min. b) The temperature changes of the tumor based on IR thermal imaging date in (a). c) Tumor growth curves of mice with various treatments including PBS control, free ^{131}I injection, CuS/I-PEG injection without or with laser irradiation, as well as CuS/[^{131}I]I-PEG injection without or with laser irradiation. d) Representative photos of tumors collected from mice at day 14 after different treatments. e) TUNEL staining of the deep region of the tumor. The combined internal RT with PTT offered remarkably enhanced therapeutic effect in inhibiting the tumor growth.

to a rather high level, which was much more significant compared to the respective monotherapy (RT alone or PTT alone). Moreover, neither death nor significantly body weight drop was noted in the different treated group (Figure S6, Supporting Information).

The mild photothermal heating triggered by a low-power NIR laser could enhance the therapeutic outcome of RT likely via a number of different mechanisms. Previous studies by our group and others have evidenced that photothermal heating to 43–45 °C may increase the cell membrane permeability and promote the cellular uptake of many NIR absorbing nanoparticles.[45,46] In addition, it is known that mild hyperthermia could increase the blood flow into the tumor and thus improve the oxygen level in the tumor microenvironment.[5] Since hypoxia would largely limit the efficacy of RT, such an effect is greatly helpful for enhancing the tumor killing ability of RT.[47] Those effects taken together may contribute to the synergistic therapeutic effect in the combined RT and PTT.

Tumor metastasis is the major cause of cancer patient death.[4] At the beginning of cancer metastasis, tumor cells usually would spread through the lymphatic circulation and reach the nearby SLNs, in which early stage metastatic sites form.[48,49] On the other hand, it is known that dye molecules or nanoparticles after being injected into solid tumors could effectively migrate into their nearby lymph nodes through lymphatic vessels.[50] We therefore wondered if we could use CuS/[^{131}I]I-PEG nanoparticles as a theranostic nanoprobe to local SLNs by multimodal imaging and treat metastasis by the combined RT and PTT. In our experiments, Balb/c mice with 4T1 tumors on their right hind paws were used 12 d after tumor inoculation to allow the development of primary tumors as well as metastatic tumors in SLNs.[31] Afterward, CuS/I-PEG nanoparticles were directly injected into the primary tumors of those mice, which were then imaged under a small animal CT scanner (**Figure 4**a). Strong CT contrast showed up as soon as at 30 min postintratumoral

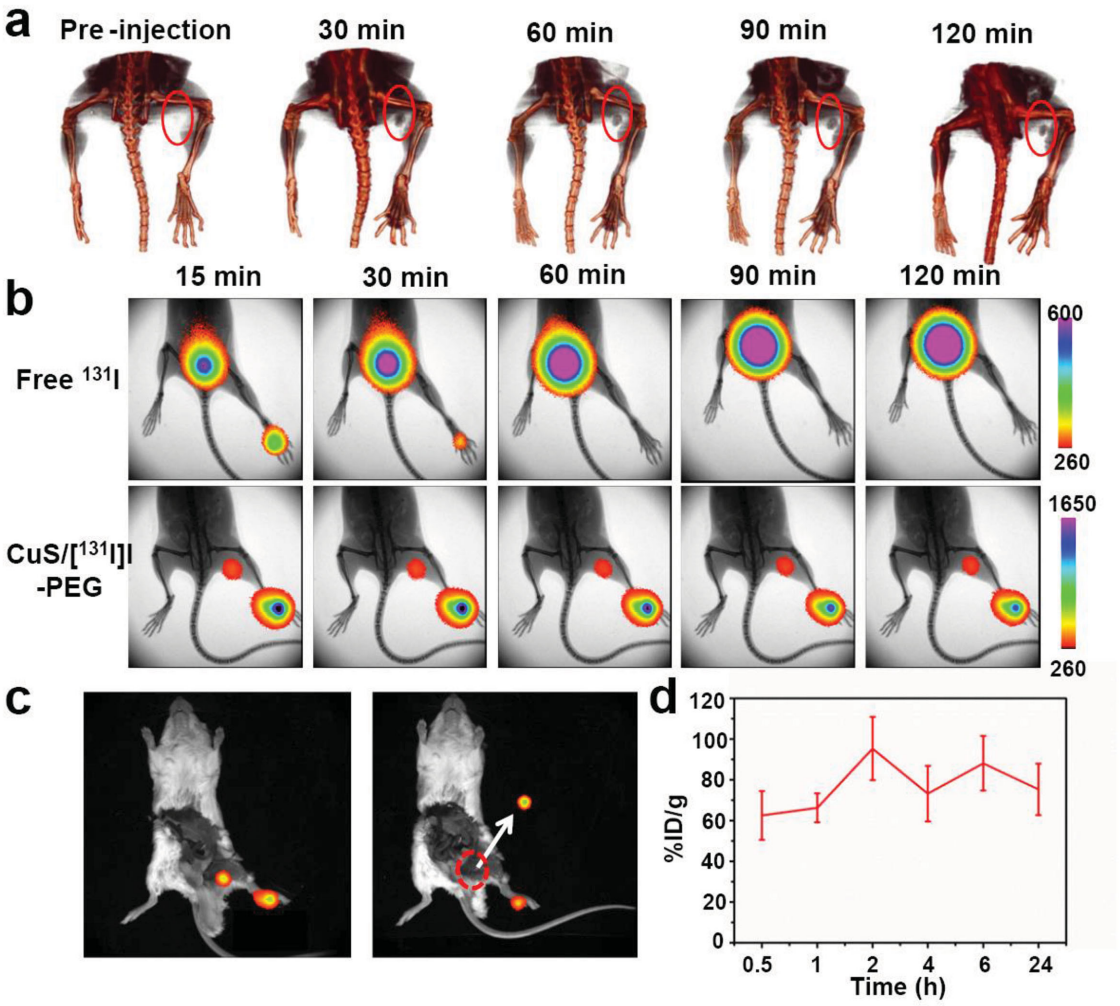

Figure 4. Multimodal imaging with CuS/[^{131}I]I-PEG for in vivo SLN mapping. a) CT imaging of mice with their primary tumors injected with CuS/I-PEG. Obvious contrast showed up in the SLNs of those mice 30 min after injection of nanoparticles. b) Gamma imaging of mice after injection of free ^{131}I or CuS/[^{131}I]I-PEG into their primary tumors on the food pads. While free ^{131}I rapidly went into the mouse bladder right after injection, CuS/[^{131}I]I-PEG nanoparticles would migrate from the injected tumor to its nearby SLN. c) Ex vivo gamma imaging of a dissected mouse to show the radioactivity signals were indeed from the lymph node. d) The lymph node uptake of CuS/[^{131}I]I-PEG at different time points postinjection of nanoparticles into primary tumors. Inset shows the photo of lymph node.

injection of CuS/I-PEG, indicating the rapid translocation of nanoparticles from the primary tumor to the nearby SLN.

^{131}I is able to emit gamma ray and could thus serve as the contrast agent in gamma imaging and single photon emission computed tomography (SPECT) imaging, the latter of which has been widely used in the clinic for whole-body 3D imaging. As we have no access to SPECT, gamma imaging was conducted to image tumor-bearing mice injected with CuS/[^{131}I]I-PEG or free ^{131}I (50 μCi per mouse). It was found that most of free ^{131}I after being injected into the tumor rapidly went into bladder by renal excretion, without showing any appreciable retention in the SLN. In contrast, strong signals appeared in the popliteal site after CuS/[^{131}I]I-PEG nanoparticles were injected into the tumor (Figure 4b). After 2 h, mice were dissected to take out the lymph node for gamma imaging. It was found that the signals in the popliteal site indeed came from the SLN (Figure 4c). For the quantitative measurement, the lymph nodes were collected at different time points post injection (p.i.) and measured by gamma counter. High SLN uptake of CuS/[^{131}I]I-PEG nanoparticles showed up as early as at 30 min p.i., and retained at high levels within 24 h (Figure 4d). Therefore, both CT and gamma imaging confirmed that CuS/[^{131}I]I-PEG after being injected into the primary tumor could effectively migrate toward the nearly SLNs, likely through lymphatic vessels.

We next would like to use the combined RT and PTT to assist surgery for the treatment of tumor metastasis (**Figure 5**a). The same lymphatic metastasis tumor model with 4T1 tumors inoculated on the right hind paws of mice was used 12 d after tumor inoculation, when metastatic tumors formed on their SLNs but not yet in other organs.[31,32] Those tumor cells if without treatment would eventually spread to other parts of the mouse body, particularly into the lung with highly enriched capillary vessels. In our experiments, different agents, including phosphate-buffered saline (PBS), free ^{131}I, CuS/I-PEG, and

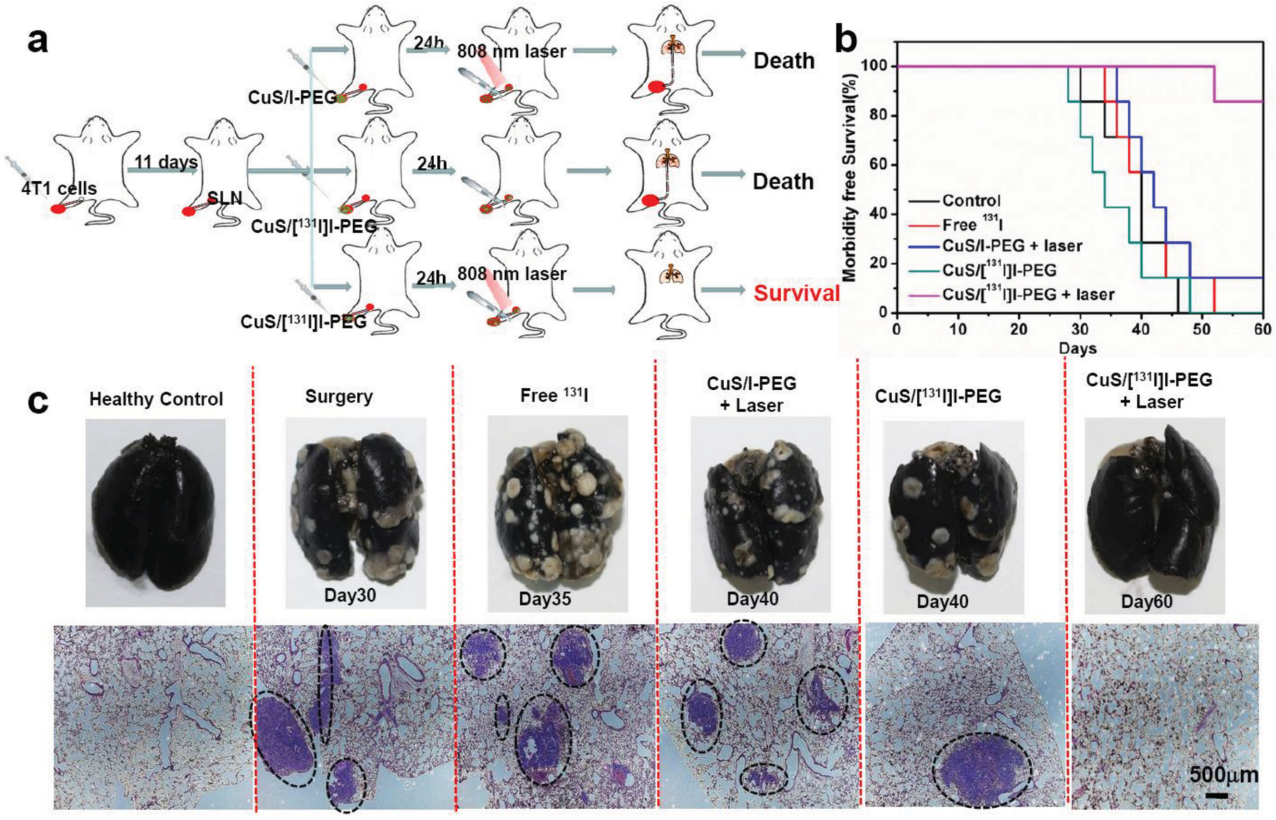

Figure 5. Combination therapy with CuS/[^{131}I]I-PEG to assist surgery in the treatment of tumor metastases. a) A scheme showing the design of our animal experiment. 4T1 cancer cells were injected into the right hind food sole of each mouse. After 12 d to allow the lymphatic metastasis, mice were randomly divided into different groups and injected with free ^{131}I, CuS/I-PEG, or CuS/[^{131}I]I-PEG into their primary tumors. PTT was conducted 2 h after injection of nanoparticles on SLNs. After 24 h, amputation was conducted to remove primary tumors on mice in all groups. b) Morbidity free survival of mice after different treatments (seven mice per group). c) Photographs of India-ink stained whole lungs and micrographs of H&E stained lung slices collected from different groups of mice. Tumor metastasis sites are highlighted by dashed circles.

CuS/[^{131}I]I-PEG, were injected into their primary tumors (CuS/I dose = 5 mg kg^{-1}, radioactivity dose = 100 μCi per mouse). For the PTT treatment, mice 2 h postinjection of CuS/I-PEG or CuS/[^{131}I]I-PEG were exposed to the 808 nm NIR laser (0.5 W cm^{-2}, 20 min), which was focused on the lymph node site of each mouse. Note that considering the lower nanoparticle concentration in the SLN compared to that directly injected into the subcutaneous tumor, a higher power density as well as a higher radioactivity dose (0.5 W cm^{-2}/100 μCi for SLN treatment vs 0.25 W cm^{-2}/50 μCi for treatment of subcutaneous tumors) was used here. As revealed by IR thermal imaging, the skin temperature on the lymph node site increased to 45–46 °C for mice injected with nanoparticles, while no significant temperature change was observed on the lymph nodes of PBS treated mice (Figure S7, Supporting Information). Therefore, it is possible to use CuS/I nanoparticles for photothermal treatment of SLNs.

To study the therapeutic benefit of the combined PTT and RT in treat tumor metastasis, a total of five groups (n = 7 per group) were included in our experiments: (1) PBS injection, (2) free ^{131}I injection, (3) CuS/I-PEG injection + laser irradiation of SLNs (PTT alone), (4) CuS/[^{131}I]I-PEG injection (RT alone), (5) CuS/[^{131}I]I-PEG injection + laser irradiation of SLNs (RT + PTT). After 24 h, surgical resection was carried out to remove the feet with the primary tumors for mice in all five groups, which were then fed in the sterile environment and closely monitored. It was found that PBS injected mice with primary tumors removed by surgery showed an average life span of ≈46 d owing to cancer metastasis. While other treated mice including RT treated by free ^{131}I, RT treated by CuS/[^{131}I]I-PEG, PTT treatment with CuS/I-PEG, all died from metastatic cancers within 52 d. Interestingly, we found that the mice treated with CuS/[^{131}I]I-PEG plus PTT treatment of SLNs showed significantly prolonged survival (only a single death within 60 d) after surgical removal of their primary tumors (Figure 5b), suggesting the superiority of the combined RT and PTT in treating lymphatic cancer metastasis to the respective mono-therapies.

According to the literature, pulmonary metastasis of cancer cells usually induced death of patients. Therefore, we should carefully examine the lungs for mice in different treatment groups. As revealed by the photo of an India-ink stained whole lungs as well as the Hematoxylin and Eosin (H&E) stained lung slices (Figure 5c), aggressive lung metastases were found in mice with their primary tumors removed by surgery, as well as those with additional RT treatment by either free ^{131}I or CuS/[^{131}I]I-PEG. For mice with surgical removal of primary tumors and photothermal heating of SLNs under our tested power density, which was a relatively mild one, lung metastasis also occurred. Excitingly, no obvious pulmonary metastasis was

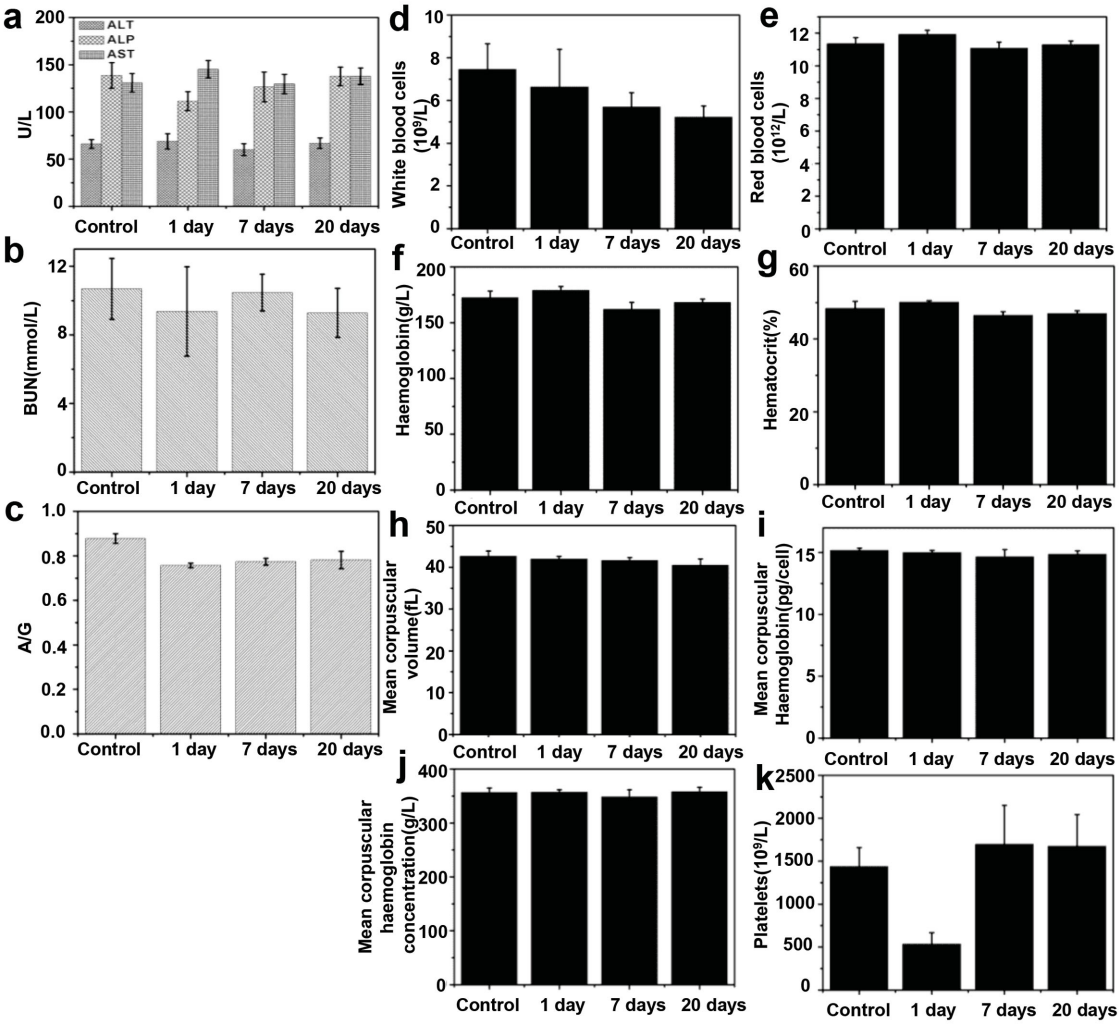

Figure 6. Blood biochemistry and hematology data of healthy female Balb/c mice treated with CuS/I-PEG at the dose of 20 mg kg^{-1} at 1, 7, and 20 d p.i. a) ALT, ALP, and AST levels in the blood at various time points after CuS/I-PEG treatment. b) Time-course albumin/globin ratios. c) Blood urea nitrogen (BUN) over time. Blood chemistry data suggested no hepatic or kidney disorder induced by CuS/I-PEG treatment. Time-course changes of white blood cells d), red blood cells e), hemoglobin f), hematocrit g), mean corpuscular volume h), mean corpuscular hemoglobin i), mean corpuscular hemoglobin concentration j), and platelets k), from control untreated mice and CuS/I-PEG treated mice. Statistic was based on five mice per data point.

observed for mice injected with CuS/[^{131}I]I-PEG plus PTT treatment of SLNs (Figure 5c), even after as long as 60 d postsurgery.

Compared with fluorescence imaging guided PTT to ablate SLNs and prevent tumor metastasis as demonstrated in our recent studies,[31,51] the current strategy presented in this work offers a number of distinctive advantages. Different from optical imaging which has limited tissue penetration depth and is only applicable for imaging of superficial SLNs, both CT and nuclear imaging, the latter of which has particularly high sensitivity, would allow whole-body 3D imaging of human patients and could be utilized to accurately determine the locations of SLNs even if they are located deeply inside the body, providing valuable information for the followed treatment planning. On the other hand, although photothermal heating of tumors to a high temperature (e.g. >50 °C throughout the whole tumor) could effective ablate cancer cells, it would certainly require a higher laser power density and may not be easily realized if SLNs with metastatic tumor cells are relatively large or covered by thick tissues. Therefore, the combination of RT with mild PTT to achieve synergistic tumor killing effect, which might be resulted from the increased cellular uptake of nanoparticles[29,30] and improved blood flow into tumors (to reverse the anaerobic environment in the tumor)[52,53] under the mild hyperthermia to enhance the efficacy RT, could have clinically meaningful advantages over RT or PTT alone with higher doses.

In order to investigate the potential in vivo toxicity of CuS/I-PEG, healthy Balb/c mice were intravenously injected with CuS/I-PEG nanoparticles at a dose of 20 mg kg^{-1}, which was fourfold of the therapy dose, and sacrificed at 1, 7, and 20 d postinjection for blood biochemistry and complete blood panel analysis ($n = 5$ per group). Age-matched healthy mice were used as a control group ($n = 5$). The liver function markers, including alanine aminotransferase (ALT), alkaline phosphatase (ALP), aspartate aminotransferase (AST), the kidney function marker urea nitrogen (BUN), as well as the albumin/globin ration, were measured to be normal (**Figure 6**a–c), suggesting no

obvious hepatic and kidney disorder of mice induced by CuS/I-PEG treatment. A complete blood panel including white blood cells, red blood cells, hemoglobin, mean corpuscular volume, mean corpuscular hemoglobin, mean corpuscular hemoglobin concentration, platelet count, and mean corpuscular hemoglobin was carried out. Compared with the control group, all parameters except the platelet count of the treated group were normal (Figure 6d–k). Although the count of platelets showed significant decrease at day 1 p.i., it recovered to the normal range after 7 and 20 d, indicating that CuS/I-PEG induced no obvious toxicity to the treated mice in the longer term. On the other hand, the major organs of mice were collected for Haematoxylin & Eosin (H&E) staining. Neither noticeable organ damage nor inflammation was observed compared with the control group (Figure S8, Supporting Information). Therefore, our synthesized CuS/I-PEG induced no significant side effect to the treated mice at least based on our short-term observation within 20 d.

3. Conclusion

In summary, radionuclide ^{131}I-doped CuS/I nanoparticles with PEG coating are fabricated in this work and used as the theranostic agent for multimodal CT/nuclear imaging and combined RT/PTT treatment. Via a one-step room temperature method, we synthesized CuS/I nanoparticles, into which ^{131}I could be easily doped with high radiolabeling stability. As demonstrated in both in vitro cell culture tests and in vivo subcutaneous tumor modal experiments, the combination of RT with PTT delivered by a single agent, CuS/[^{131}I]I-PEG, offered remarkable synergistic therapeutic effect compared to RT or PTT alone. We further applied such nanoagent for imaging and treatment of lymphatic tumor metastasis. By using the radioactivity and X-ray absorbing ability of CuS/[^{131}I]I-PEG, in vivo gamma imaging and CT imaging was conducted, revealing the rapid and efficiency translocation of those nanoparticles from the injected primary tumors to the nearby SLNs. Importantly, it was further demonstrated that surgical removal of primary tumors assisted with combined RT and PTT treatment of SLNs with CuS/[^{131}I]I-PEG could effectively prevent further tumor metastasis and dramatically prolong the survival of animals. Moreover, no significant in vivo toxicity was found for those CuS/I-PEG nanoparticles at a high dose within 20 d. Therefore, the combination of internal RT with PTT is for the first time realized in this work with a novel nanoagent, which in the meantime enables multimodal imaging to help the treatment planning. Moreover, our proposed new cancer treatment strategy, the imaging-guided combined RT & PTT treatment of SLNs to assist surgery, may have clinical values in the treatment of tumor metastasis.

4. Experimental Section

Preparation of PEGylated CuS/I Nanoparticles: CuS/I nanoparticles were synthesized following our previous reported protocol used for the fabrication of bare CuS nanoparticles with slight modifications.[44] Briefly, 14 mg of copper (II) chloride ($CuCl_2.2H_2O$) and 20 mg of sodium citrate were mixed and dissolved in 100 mL of deionized water under magnetic stirring at room temperature. 5 min later, 3.9 mg of sodium sulfide(Na_2S) and 1.66 mg of potassium iodide (KI) was added to the mixed solution dropwise. The mixture was reacted at room temperature overnight. The citrate-coated CuS/I nanoparticles were obtained. In order to modify CuS/I nanoparticles, PEG grafted poly(maleic anhydride-alt-1-octadecene) (C18PMH-PEG) and amine-terminated C18PMH-PEG (C18PMH-PEG-NH_2) were synthesized according to our previously published procedure[54] and used to modify noncovalent CuS/I nanoparticles. For PEGylation of CuS/I nanoparticles, 50 mg of C18-PMH-PEG or C18PMH-PEG-NH_2 (when used for fluorescent labeling) polymer was added to the above-mentioned mixture directly and then sonicated for 90 min. After 6 h of stirring, the obtained PEGylated CuS/I nanoparticles were washed for several times by ultrafiltration filters with molecular weight cutoff (MWCO) of 100 kDa to remove excess reagents. The final product was stored in 4 °C for next experiments.

Synthesis of ^{131}I-Doped CuS (CuS/[^{131}I]I) NPs: PEGylated CuS/[^{131}I]I-PEG NPs were synthesized as described in the preceding section with a trace amount of Na^{131}I (about 10 mCi) in addition to potassium iodide (KI). Free ^{131}I was removed by centrifuge filtration through Amicon centrifugal filters (MWCO = 10 kDa) and washed with water for six times. The radio-doped efficiency was tested by adding different molar ratio of $CuCl_2$, Na_2S, KI, and Na^{131}I. The doped ^{131}I was measured by gamma count. For radio-stability examination, 50 µL of CuS/[^{131}I]I-PEG (500 µg mL^{-1}) was mixed with 450 µL of mouse plasma at 37 °C in a water bath. Free ^{131}I was removed by centrifuge filtration through Amicon centrifugal filters (MWCO = 10 kDa) at different time points. The leftover CuS/[^{131}I]I-PEG after washing with water three times was collected for gamma counting to measure the amount of retained ^{131}I on the nanoparticles.

Cellular Experiments: The 4T1 murine breast cancer cell line was originally obtained from American Type Culture Collection (ATCC) and cultured under recommended conditions. To determine the cellular uptake efficiencies, 4T1 cells preseeded in six-well plates at the density of 2×10^5 cells/well were incubated with 30 mg mL^{-1} of FITC labeled CuS/I-PEG for different periods of time (0.5, 2, 4, 6 h). After washing cells with phosphate buffered saline (PBS) for three times, cells were tested by flow cytometry. After 6 h incubation, the cells were stained with 4′,6-diamidino-2-phenylindole (DAPI) and then imaged by a laser scanning confocal fluorescence microscope (Leica SP5). For in vitro RT, 4T1 cells preseeded into 96-well plates were incubated with different concentrations of CuS/[^{131}I]I-PEG, CuS/I-PEG, and free ^{131}I for 24 h. Relative cell viabilities were determined by the cell counting kit (CCK-8) assay. For in vitro combined therapy, 4T1 cells were incubated with CuS/[^{131}I]I-PEG (30 mg mL^{-1} of CuS/I-PEG corresponding to 120 mCi mL^{-1} of ^{131}I), CuS/I-PEG (30 µg mL^{-1}), or free ^{131}I (120 µCi mL^{-1}). After 12 h of incubation, cells were irradiated by an 808 nm laser at 0.8 W cm^{-2} for 5 min. Relative cell viabilities were determined after another 12 h of incubation by the CCK-8 assay. Meanwhile, cells after different treatments were stained with calcine AM/prodium iodide (PI) for 30 min to distinguish live cells (green color) and dead cells (red color), and then imaged by a confocal fluorescence microscope (OLYMPUS, IX73).

Combination Therapy on the Subcutaneous Tumor Model: Female Balb/c mice were obtained from Nanjing Peng Sheng Biological Technology Co. Ltd and used under protocols approved by the Soochow University Laboratory Animal Center. 2×10^6 4T1 cells suspended in 60 µL phosphate buffered saline (PBS) were subcutaneously injected into the right shoulder of each mouse. The mice bearing 4T1 tumors were treated when the tumor volume reached ≈100 mm^3. To evaluate the combined therapeutic effect in vivo, mice were randomly divided into six groups (n = 5 per group) for various treatments including untreated group, mice intratumorally injected with 50 µL of free ^{131}I (50 µCi per mouse), mice intratumorally injected with 50 µL of CuS/I-PEG with and without laser irradiation (5 mg kg^{-1} per mouse), and mice intratumorally injected with 50 µL of CuS/[^{131}I]I-PEG with and without laser irradiation (50 µCi per mouse). After 24 h postinjection (p.i.), tumors of mice treated with CuS/I-PEG and CuS/[^{131}I]I-PEG were irradiated by the 808 nm NIR laser at a power density of 0.25–0.3 W cm^{-2} to maintain the tumor temperature at about 45–46 °C for 20 min under the monitoring by a infrared camera (FLIR E50) . The tumor sizes and body weights

were monitored every 2 d. The tumor volume was calculated according to the following equation: volume = width^2 × length/2. Relative tumor volumes were calculated as V/V_0 (V_0 was the tumor volume when the treatment was initiated). On the other hand, tumors tissue from all six treated group were collected 1 d posttreatment for TUNEL staining (Roche) and examined by a fluorescence microscope (Olympus).

Blood Chemistry Analysis and Histology Examinations: Fifteen healthy Blab/c mice randomly divided into three groups (five mice in each group) were intravenous injected with CuS/I-PEG at a dose of 20 mg kg^{-1} and sacrificed at 1, 7, and 15 d p.i., respectively. Another five healthy mice without treated with CuS/I-PEG were used as control group. Blood (≈0.8 mL) was drawn from those mice for blood biochemistry examination. Meanwhile, major organs including liver, spleen, kidney, heart, lung were collected, fixed in 4% formalin, conducted with paraffin embedded sections, stained with Hematoxylin and Eosin (H&E), and examined under a digital microscope (Olympus).

Lymph Node Metastases Imaging: 1×10^6 4T1 cells suspended in 40 µL of PBS solution was injected subcutaneously on the right hind foot sole of Balb/c mice. At day 12 posttumor inoculation, we selected mice that had spherical hard lumps in their inner knee for our next experiments. Mice bearing 4T1 tumors treated with free ^{131}I (50 µCi per mouse) or CuS/I-PEG (30 mg kg^{-1} of CuS/[^{131}I]I-PEG corresponding to 50 µCi of ^{131}I per mouse) were imaged by an in vivo animal imaging system (Kodak, FX Pro) and a small animal CT imaging system (TriFoil Imaging, Inc.) at various time points. Meanwhile, the lymph nodes uptake of CuS/[^{131}I]I-PEG was measured by the gamma counter.

Combined Therapy in Lymphatic Metastatic Tumor Model: To evaluate the combined therapeutic effects on lymph node metastasis, the mice were randomly divided into five groups (n = 7 per group) including: (1) PBS injection, (2) free ^{131}I injection, (3) CuS/I-PEG injection + laser irradiation of SLNs (PTT alone), (4) CuS/[^{131}I]I-PEG injection (RT alone), (5) CuS/[^{131}I]I-PEG injection + laser irradiation of SLNs (RT + PTT). PTT was carried out by irradiating the SLN sites using the 808 nm laser at 0.5 W cm^{-2} for 20 min. All the primary tumors of mice were removed 24 h after treatment by surgical dissection of their feet with tumors.

Examination of Lung Metastasis: To examine lung metastasis, mice after various treatments were sacrificed at desired time points right after India ink (15%) was injected into their lungs through the trachea. Their lungs were collected and soaked in a Fekete's solution (100 mL of 70% alcohol, 10 mL formalin, and 5 mL glacial acetic acid) at room temperature for 2–3 d and then photographed. White spots on the black-stained lungs were tumor metastasis sites. For histology examination, lungs from different groups of mice were harvested, fixed in 10% formalin, processed routinely into paraffin, sectioned at 8 µm thickness, and stained with Hematoxylin & Eosin (H&E).

Supporting Information

Supporting Information is available from the Wiley Online Library or from the author.

Acknowledgements

This work was partially supported by the National Basic Research Program of China (973 Program 2014CB931900, 2012CB932600), National Natural Science Foundation of China (81471716, 81302383, 31400861, 21207164, 51222203), the National Natural Science Foundation of Jiangsu Province (BK20140320, BK20130005), and a Project Funded by the Priority Academic Program Development of Jiangsu Higher Education Institutions (PAPD).

Received: May 14, 2015
Published online: June 22, 2015

[1] Z. Zhang, J. Wang, C. Chen, *Adv. Mater.* **2013**, *25*, 3869.
[2] D. Peer, J. M. Karp, S. Hong, O. C. FaroKhzad, R. Margalit, R. Langer, *Nat. Nanotech.* **2007**, *2*, 751.
[3] M.-E. Bonnet, J.-B. Gossart, E. Benoit, M. Messmer, O. Zounib, V. Moreau, J.-P. Behr, N. Lenne-Samuel, V. Kedinger, A. Meulle, P. Erbacher, A.-L. Bolcato-Bellemin, *J. Controlled Release* **2013**, *170*, 183.
[4] S. Valastyan, R. A. Weinberg, *Cell* **2011**, *147*, 275.
[5] K. F. Chu, D. E. Dupuy, *Nat. Rev. Cancer* **2014**, *14*, 199.
[6] L. Cheng, C. Wang, L. Feng, K. Yang, Z. Liu, *Chem. Rev.* **2014**, *114*, 10869.
[7] X. H. Huang, I. H. El-Sayed, W. Qian, M. A. El-Sayed, *J. Am. Chem. Soc.* **2006**, *128*, 2115.
[8] M. C. Daniel, D. Astruc, *Chem. Rev.* **2004**, *104*, 293.
[9] J. Perez-Juste, I. Pastoriza-Santos, L. M. Liz-Marzan, P. Mulvaney, *Coord. Chem. Rev.* **2005**, *249*, 1870.
[10] E. B. Dickerson, E. C. Dreaden, X. Huang, I. H. El-Sayed, H. Chu, S. Pushpanketh, J. F. McDonald, M. A. El-Sayed, *Cancer Lett.* **2008**, *269*, 57.
[11] L. Tong, Q. Wei, A. Wei, J.-X. Cheng, *Photochem. Photobiol.* **2009**, *85*, 21.
[12] J. Chen, D. Wang, J. Xi, L. Au, A. Siekkinen, A. Warsen, Z.-Y. Li, H. Zhang, Y. Xia, X. Li, *Nano Lett.* **2007**, *7*, 1318.
[13] M. Chen, S. Tang, Z. Guo, X. Wang, S. Mo, X. Huang, G. Liu, N. Zheng, *Adv. Mater.* **2014**, *26*, 8210.
[14] P. Huang, J. Lin, W. Li, P. Rong, Z. Wang, S. Wang, X. Wang, X. Sun, M. Aronova, G. Niu, R. D. Leapman, Z. Nie, X. Chen, *Angew. Chem. Int. Ed.* **2013**, *52*, 13958.
[15] K. Yang, S. Zhang, G. Zhang, X. Sun, S.-T. Lee, Z. Liu, *Nano Lett.* **2010**, *10*, 3318.
[16] K. Yang, L. Feng, X. Shi, Z. Liu, *Chem. Soc. Rev.* **2013**, *42*, 530.
[17] D. Bitounis, H. Ali-Boucetta, B. H. Hong, D. H. Min, K. Kostarelos, *Adv. Mater.* **2013**, *25*, 2258.
[18] Q. Tian, J. Hu, Y. Zhu, R. Zou, Z. Chen, S. Yang, R. Li, Q. Su, Y. Han, X. Liu, *J. Am. Chem. Soc.* **2013**, *135*, 8571.
[19] T. Liu, C. Wang, X. Gu, H. Gong, L. Cheng, X. Shi, L. Feng, B. Sun, Z. Liu, *Adv. Mater.* **2014**, *26*, 3433.
[20] L. Cheng, J. Liu, X. Gu, H. Gong, X. Shi, T. Liu, C. Wang, X. Wang, G. Liu, H. Xing, W. Bu, B. Sun, Z. Liu, *Adv. Mater.* **2014**, *26*, 1886
[21] Q. Tian, M. Tang, Y. Sun, R. Zou, Z. Chen, M. Zhu, S. Yang, J. Wang, J. Wang, J. Hu, *Adv. Mater.* **2011**, *23*, 3542.
[22] Q. Tian, F. Jiang, R. Zou, Q. Liu, Z. Chen, M. Zhu, S. Yang, J. Wang, J. Wang, J. Hu, *ACS Nano* **2011**, *5*, 9761.
[23] K. Yang, H. Xu, L. Cheng, C. Sun, J. Wang, Z. Liu, *Adv. Mater.* **2012**, *24*, 5586.
[24] Z. Zha, X. Yue, Q. Ren, Z. Dai, *Adv. Mater.* **2013**, *25*, 777.
[25] Z. S. Al-Ahmady, O. Chaloin, K. Kostarelos, *J. Controlled Release* **2014**, *196*, 332.
[26] J. F. Lovell, C. S. Jin, E. Huynh, H. Jin, C. Kim, J. L. Rubinstein, W. C. W. Chan, W. Cao, L. V. Wang, G. Zheng, *Nat. Mater.* **2011**, *10*, 324.
[27] Z. Sheng, D. Hu, M. Zheng, P. Zhao, H. Liu, D. Gao, P. Gong, G. Gao, P. Zhang, Y. Ma, L. Cai, *ACS Nano* **2014**, *8*, 12310.
[28] L. Feng, K. Li, X. Shi, M. Gao, J. Liu, Z. Liu, *Adv. Health Mater.* **2014**, *3*, 1261.
[29] L. Feng, X. Yang, X. Shi, X. Tan, R. Peng, J. Wang, Z. Liu, *Small* **2013**, *9*, 1989.
[30] B. Tian, C. Wang, S. Zhang, L. Feng, Z. Liu, *ACS Nano* **2011**, *5*, 7000.
[31] C. Liang, S. Diao, C. Wang, H. Gong, T. Liu, G. Hong, X. Shi, H. Dai, Z. Liu, *Adv. Mater.* **2014**, *26*, 5646.
[32] Q. Chen, C. Liang, X. Wang, J. He, Y. Li, Z. Liu, *Biomaterials* **2014**, *35*, 9355.
[33] Y. Li, W. Lu, Q. Huang, M. Huang, C. Li, W. Chen, *Nanomedicine* **2010**, *5*, 1161.

[34] G. Ku, M. Zhou, S. Song, Q. Huang, J. Hazle, C. Li, *ACS Nano* **2012**, *6*, 7489.
[35] Z. Zha, S. Zhang, Z. Deng, Y. Li, C. Li, Z. Dai, *Chem. Commun.* **2013**, *49*, 3455.
[36] L. Guo, D. D. Yan, D. Yang, Y. Li, X. Wang, O. Zalewski, B. Yan, W. Lu, *ACS Nano* **2014**, *8*, 5670.
[37] L. Zhang, S. Gao, F. Zhang, K. Yang, Q. Ma, L. Zhu, *ACS Nano* **2014**, *8*, 12250.
[38] X. Ding, C. H. Liow, M. Zhang, R. Huang, C. Li, H. Shen, M. Liu, Y. Zou, N. Gao, Z. Zhang, Y. Li, Q. Wang, S. Li, J. Jiang, *J. Am. Chem. Soc.* **2014**, *136*, 15684.
[39] S. Goel, F. Chen, W. Cai, *Small* **2014**, *10*, 631.
[40] J. Bai, Y. Liu, X. Jiang, *Biomaterials* **2014**, *35*, 5805.
[41] Q. Xiao, X. Zheng, W. Bu, W. Ge, S. Zhang, F. Chen, H. Xing, Q. Ren, W. Fan, K. Zhao, Y. Hua, J. Shi, *J. Am. Chem. Soc.* **2013**, *135*, 13041.
[42] M. Zhou, R. Zhang, M. Huang, W. Lu, S. Song, M. P. Melancon, M. Tian, D. Liang, C. Li, *J. Am. Chem. Soc.* **2010**, *132*, 15351.
[43] S. Wang, A. Riedinger, H. Li, C. Fu, H. Liu, L. Li, T. Liu, L. Tan, M. J. Barthel, G. Pugliese, F. D. Donato, M. S. D'Abbusco, X. Meng, L. Manna, H. Meng, T. Pellegrino, *ACS Nano* **2015**, *9*, 1788.
[44] K. Yang, L. Zhu, L. Nie, X. Sun, L. Cheng, C. Wu, G. Niu, X. Chen, Z. Liu, *Theranostics* **2014**, *4*, 134.
[45] S. P. Sherlock, S. M. Tabakman, L. M. Xie, H. J. Dai, *ACS Nano* **2011**, *5*, 1505.
[46] T. Liu, C. Wang, W. Cui, H. Gong, C. Liang, X. Z. Shi, Z. W. Li, B. Q. Sun, Z. Liu, *Nanoscale* **2014**, *6*, 11219.
[47] Y. Y. Liu, Y. Liu, W. B. Bu, Q. F. Xiao, Y. Sun, K. L. Zhao, W. P. Fan, J. N. Liu, J. L. Shi, *Biomaterials* **2015**, *49*, 1.
[48] M. Skobe, T. Hawighorst, D. G. Jackson, R. Prevo, L. Janes, P. Velasco, L. Riccardi, K. Alitalo, K. Claffey, M. Detmar, *Nat. Med.* **2001**, *7*, 192.
[49] T. P. Padera, A. Kadambi, E. di Tomaso, C. M. Carreira, E. B. Brown, Y. Boucher, N. C. Choi, D. Mathisen, J. Wain, E. J. Mark, L. L. Munn, R. K. Jain, *Science* **2002**, *296*, 1883.
[50] Y. W. Noh, S. H. Kong, D. Y. Choi, H. S. Park, H. K. Yang, H. J. Lee, H. C. Kim, K. W. Kang, M. H. Sung, Y. T. Lim, *ACS Nano* **2012**, *6*, 7820.
[51] Q. Chen, C. Liang, C. Wang, Z. Liu, *Adv. Mater.* **2015**, *27*, 903.
[52] G. Kong, R. D. Braun, M. W. Dewhirst, *Cancer Res.* **2000**, *60*, 4440.
[53] M. P. Melancon, A. M. Elliott, A. Shetty, Q. Huang, R. J. Stafford, C. Li, *J. Controlled Release* **2011**, *156*, 265.
[54] X. Liu, H. Tao, K. Yang, S. Zhang, S.-T. Lee, Z. Liu, *Biomaterials* **2011**, *32*, 144.